Journal of Membrane Science 695 (2024) 122467

Contents lists available at ScienceDirect

Journal of Membrane Science

journal homepage: www.elsevier.com/locate/memsci

Homoporous membranes of block copolymers: Upscalable preparation by spray coating and performance boosting by quaternization

Jiemei Zhou [a], Yifei Huang [a], Can Chen [a], Yong Wang [a,b,*]

[a] State Key Laboratory of Materials-Oriented Chemical Engineering, College of Chemical Engineering, Nanjing Tech University, Nanjing, 211816, Jiangsu, China
[b] School of Energy and Environment, Southeast University, Nanjing, 210096, Jiangsu, China

ARTICLE INFO

Keywords:
Homoporous membranes (HOMEs)
Block copolymers (BCPs)
Spray coating
Selective swelling
Membrane separation

ABSTRACT

The remarkable permselectivity of homoporous membranes (HOMEs) confers them with unparalleled advantages in high-precision separation. However, the upscalable fabrication of HOMEs remains a challenging yet crucial task to meet practical demands. Herein, we present a facile and controllable strategy for producing HOMEs through spray coating of block copolymers (BCPs) on macroporous substrates, followed by annealing and selective swelling. By controlling the BCP concentrations and ambient humidity during spray coating, dense BCP layers with adjustable thickness can be formed. The use of suitable pore-filling agents for filling the pores of substrates during spray coating and annealing prevents BCP from penetrating into the substrates. Also, it ensures robust adhesion between the BCP layers and macroporous substrates. Direct spray-coating circumvents the intricate and uncontrollable BCP layer transformation process, thereby enabling the successful fabrication of HOMEs over a large area of 100 cm^2. The separation performances of thus-prepared homoporous membranes can be easily regulated by changing the swelling durations. Furthermore, the selective swelling process leads to the enrichment of BCP polarity chains on the surface and pore walls, allowing for further quaternization modification. Consequently, a synchronous promotion in permeability and selectivity of HOMEs is achieved.

1. Introduction

The pore structures, including pore size, uniformity, pore type, porosity, etc., play a pivotal role in determining the separation performance of a membrane [1–3]. With the ever-expanding applications of membrane separation technology in various fields, there is an increasing demand for higher selectivity and permeability for membranes, which drives the development of porous structures toward greater regularity, refinement, and controllability [4,5]. Homoporous membranes (HOMEs) are characterized by uniform pore sizes, same pore geometries, and vertically aligned through pores [6,7]. Uniform pore sizes allow for more precise screening of materials with varying sizes, ensuring sharp selectivity. Meanwhile, straight-through porosities shorten the passage channels and minimize mass transfer resistance, leading to ultrafast permeability. These advantages of HOMEs over conventional membranes with tortuous porosities and scattered apertures enable them to meet the demand of high-precision separation applications, such as protein and peptide classification, virus removal, pharmaceutical purification, etc [8–11]. The design and preparation of HOMEs have thus emerged as a pivotal research focus in the field of membrane separation.

In regard to the preparation of HOMEs, block copolymers (BCPs) have garnered significant attention due to their special microphase separation property [12–14]. BCPs are a class of fascinating materials comprising two or more covalently linked chains with distinct repeating units. Due to the thermodynamic incompatibility between different chains, BCPs can undergo microphase separation through different annealing techniques, such as thermal annealing, solvent annealing, microwave annealing and laser annealing [15–18], resulting in the formation of long-range ordered nanopatterns [19–21]. Among these nanopatterns, the one with cylindrical phases of the minority blocks perpendicularly aligned within the matrix of the majority blocks offers an ideal design platform for the preparation of HOMEs [22,23]. Chemical etching of the minority blocks or extraction of the predosed additives incorporated into cylindrical phases are the direct ways to produce straight-through porosities from BCPs [24–27]. Sequential infiltration synthesis (SIS) to selectively grow inorganic species within the matrix of the majority blocks, followed by etching of BCPs, could result in the

* Corresponding author. State Key Laboratory of Materials-Oriented Chemical Engineering, College of Chemical Engineering, Nanjing Tech University, Nanjing, 211816, Jiangsu, China.
E-mail address: yongwang@seu.edu.cn (Y. Wang).

https://doi.org/10.1016/j.memsci.2024.122467
Received 10 November 2023; Received in revised form 16 January 2024; Accepted 18 January 2024
Available online 23 January 2024

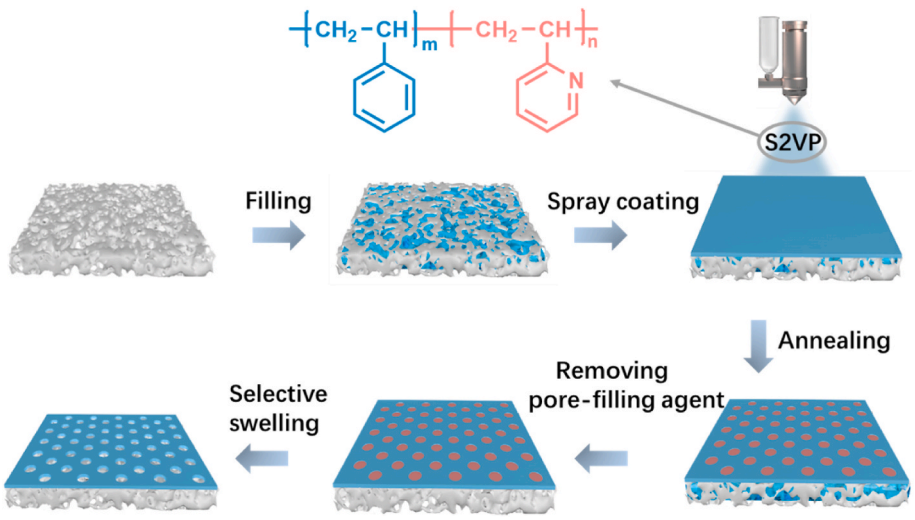

Fig. 1. The schematic diagram of the preparation process of HOMEs.

inorganic HOMEs [28–30]. Nevertheless, these pore-making approaches are destructive to the ordered BCPs and are considerably laborious. To overcome the limitations, we have developed a nondestructive and ease-to-operate method for generating pores in phase-separated BCPs, which is called selective swelling-induced pore generation [31–33]. By selective swelling of minority phases in an appropriate solvent and subsequent drying, well-defined pores can be generated without damaging the BCP precursors. Importantly, the pore sizes can be flexibly tuned by changing the swelling parameters. Thus, this highly convenient method has been widely utilized in the fabrication of HOMEs with diverse pore sizes [34].

In consideration of the exorbitant expenses and inadequate mechanical strength of BCP materials, HOMEs from BCPs are usually in the form of composite membranes with homoporous BCP layers atop the macroporous substrates [35]. Typically, BCPs are first coated on dense substrates of silicon wafers or glass plates to form thin films. After annealing to perpendicularly align their microphase-separated structures, the BCP films are detached from dense substrates and transferred onto the porous substrates to prepare HOMEs [36–38]. However, the detachment and transformation procedures necessitate laborious and meticulous operations to avert damage to the delicate thin BCP layers, thereby restricting this approach only viable to small-sized fabrication, typically less than 10 cm^2 [7]. Besides, the rough composite process of attaching BCP layers onto substrates cannot guarantee sufficient interlayer adhesion, which could have a negative impact on the performance stability of the membranes upon long-term use and impede the possibility of further modification to adapt specific applications. Recently, our group has reported the manufacturing of HOMEs using the BCP of polystyrene-*block*-poly(2-vinyl pyridine) (PS-*b*-P2VP, abbreviated as S2VP), with an extended membrane area of up to 100 cm^2 [39]. Whereas, the current study still relies on the detachment and transformation process, which fails to address existing issues fundamentally. Additionally, multiple annealing is required to achieve hexagonally arranged ordering. Therefore, there is a high demand for innovative scalable methods for the fabrication of HOMEs with large areas.

In this work, we utilized the spray-coating method to directly deposit S2VP onto macroporous substrates. Subsequent annealing of as-coated membranes in a saturated chloroform vapor environment facilitated the perpendicular alignment of P2VP microdomains within the S2VP layers. Swelling the aligned S2VP layers in hot ethanol enabled the formation of ordered through pores and ultimately yielded HOMEs. Pore-filling agents were used to fill the macropores of substrates in order to prevent S2VP from penetrating into the substrates during spray coating and annealing. It was found that the pore-filling agents had a great impact on the pore morphology and interlayer adhesive strength. By selecting an appropriate pore-filling agent, we successfully fabricated HOMEs with strong interlayer adhesion in a large area of 100 cm^2. The HOMEs exhibited excellent separation performances and could be further enhanced in both permeability and selectivity through quaternization modification.

2. Experimental section

2.1. Materials

S2VP (M_n^{PS} = 290 kDa, M_n^{P2VP} = 72 kDa, polydispersity index (PDI) = 1.10) was bought from Polymer Source Inc. The hydrophilic polyvinylidene fluoride (PVDF) membranes as the porous substrates (average pore diameter of 0.22 μm) were purchased from Haining Yibo Filtration Equipment Co., Ltd. Polyvinyl alcohol (PVA, M_w = 1750 Da) was obtained from Shanghai Lingfeng Chemical Reagent Co., Ltd. Poly (sodium *p*-styrenesulfonate) (PSS, M_w = 80 kDa, 20 wt% aqueous solutions) was purchased from Shanghai Macklin Biochemical Co., Ltd. Polyethylene glycol (PEG, M_w = 3.6~4.4 kDa) and polyvinyl pyrrolidone (PVP, M_w = 44–54 kDa) were bought from Sinopharm Chemical Reagent Co., Ltd. Monodispersed gold nanoparticles in water (diameters of 15 nm and 5 nm) were obtained from BBI Solutions. Other reagents including chloroform (≥99 %), ethanol (≥99.7 %), and bromoethane (≥99 %) were provided by Shanghai Aladdin Biochemical Technology Co., Ltd.

2.2. Membrane preparation

S2VP was ultrasonically dissolved in chloroform to prepare the membrane-casting solutions with varying concentrations, and the obtained solutions were filtered three times through polytetrafluoroethylene (PTFE) filters to remove any impurities. PVA, PSS, PEG, or PVP were dissolved in water, and obtained solutions with different concentrations were used as pore-filling agents. The process of membrane preparation is illustrated in Fig. 1. A piece of 10 cm × 10 cm PVDF membrane was placed on the liquid surface of the pore-filling agent letting the pore-filling agent penetrate into and fill the pores of the membrane. After being filled, the PVDF membrane was placed on the plate of the spray device (SEV-300EDN, Suzhou Second Automatic Equipment Co., Ltd). Then, the S2VP solution was spray-coated onto the surface of the PVDF membrane with 1 bar of compressed air. The spray device was positioned within a fume hood with the ambient humidity controlled at 20–50 %. The spray nozzle was maintained 62 mm higher

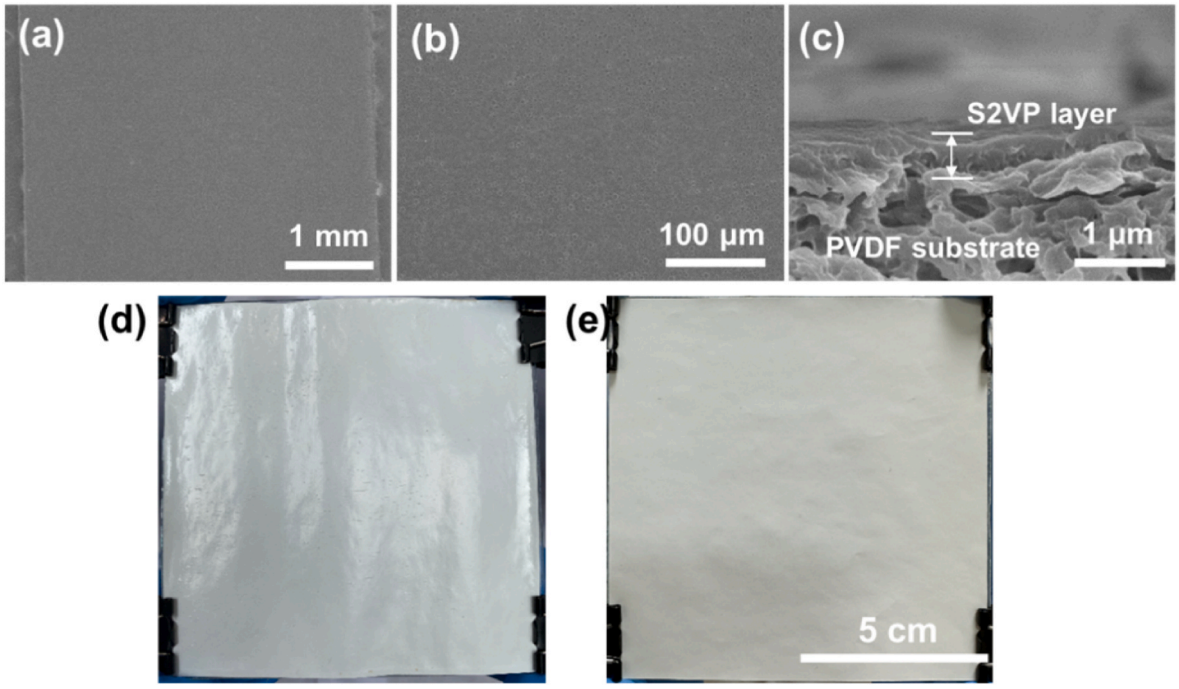

Fig. 2. The composite membrane fabricated with an S2VP concentration of 0.5 wt%. The surface SEM images (a) at low magnification and (b) at high magnification. (c) The cross-sectional SEM image. Digital images of (d) the S2VP coated side and (e) the PVDP substrate side. Images of (d) and (e) have the same magnification with a scale bar corresponding to 5 cm provided in (e).

than the plate, and the spray coating process was repeated until the S2VP solution in the reservoir of the spray device was exhausted. After spray coating, the obtained composite membrane was dried naturally at room temperature until the residual chloroform solvent in the S2VP layer evaporated completely. Before annealing, the composite membrane was placed onto the liquid surface of the pore-filling agent again for 10 min to replenish it. An S2VP film coated on the silicon wafer was used as a reference to monitor the annealing process since we needed to observe the color change during the process. The annealing process was carried out in a 450 mL container equipped with a glass platform. 100 mL chloroform was added to the container, then the composite membrane and the reference were placed on the platform at the same time, followed by sealing the container immediately to allow a saturated chloroform vapor environment for annealing. When the color of the reference turned green, the container was opened to release the saturated chloroform vapor and stop the annealing process. After that, in order to remove the pore-filling agents of PSS, PEG, or PVP inside the pores of PVDF, the composite membrane was immersed in pure water at room temperature with stirring at 300 rpm for 2 h, while for removing PVA, the composite membrane was soaked in pure water at 90 °C for 2 h. Then, the composite membrane was immersed in ethanol at 65 °C for different durations to create homoporous structure in the S2VP layer by the selective swelling-induced pore generation process. After undergoing selective swelling and natural drying, the HOME was finally obtained.

A further modification was conducted by soaking the prepared HOME in the bromoethane-ethanol mixed solvent containing 5 % or 10 % bromoethane (v/v) at room temperature for 1–12 h, then taking the membrane out from the solvent and allowing it to dry naturally.

2.3. Characterizations

A filed-emission scanning electron microscope (FE-SEM, Hitachi S-4800) was used to characterize the morphologies of HOMEs at an accelerating voltage of 3-5 kV. For cross-sectional observation, HOMEs were immersed in isopropanol to fill the pores, then immersed in liquid nitrogen for quick freezing followed by rupturing to expose the cross sections. All samples were sputter-coated with a gold layer to improve conductivity before SEM characterizations. The Br contents of the composite membranes were analyzed by the energy-dispersive *X*-ray (EDX) spectrometer (Noran) at an accelerating voltage of 20 kV. The surface hydrophilicity of membranes was detected by an angle goniometer (DropMeter A-100, Maist), and at least 5 positions of each sample should be measured to afford the average value of the water contact angle.

2.4. Membrane filtration tests

A dead-end filtration device (Amicon 8003, Merck Millipore) was used to assess the separation performances of HOMEs under a pressure of 0.8 bar. Before measurements, the membrane was pre-compacted under the same pressure for 10 min in order to achieve a stable filtration state. The water permeance (P, L • m^{-2} • h^{-1} • bar^{-1}) was calculated by Eq. (1):

$$P = \frac{V}{A \bullet t \bullet \Delta p} \tag{1}$$

where V (L) represents the volume of water passing through the membrane during the testing period t (h), A (m^2) denotes the effective filtration area, and Δp (bar) indicates the applied testing pressure.

Monodisperse gold nanoparticles with sizes of 5 nm and 15 nm were used for rejection tests. Before tests, the HOMEs were immersed in a solution of Acid Orange 7 (5 mg • L^{-1}) for 20 min to neutralize the membrane surface in case of the surface adsorption of gold nanoparticles [40]. UV–vis spectrophotometry (NanoDrop 2000c, Thermo Fisher Scientific) was used to analyze the concentrations of gold nanoparticles in the feed, permeation, and retentate solutions. The rejection rates were calculated by Eq. (2):

$$R = 1 - \frac{C_p}{C_f} \times 100\% \tag{2}$$

where C_p (g • L^{-1}) and C_f (g • L^{-1}) represent the concentrations of gold

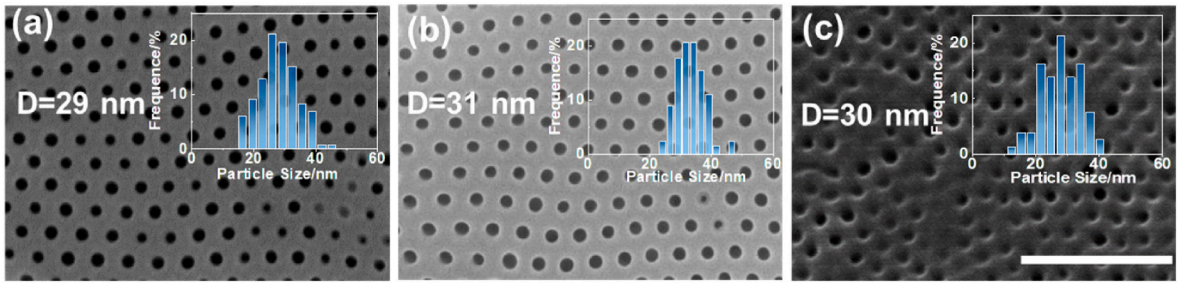

Fig. 3. The surface SEM images of membranes fabricated with different S2VP concentrations after swelling at 65 °C for 5 h: (a) 5 wt%, (b) 7.5 wt%, and (c) 1 wt%. Insets show the pore size distribution and the average pore size of the corresponding membranes. Images have the same magnification with a scale bar corresponding to 500 nm provided in (c).

nanoparticles in the permeation and the feed solutions, respectively.

3. Results and discussion

3.1. Effects of the membrane-casting solution concentrations

The membrane-casting solutions with different S2VP concentrations were investigated in order to form a dense BCP layer without noticeable defects atop the porous substrate during spray coating. We fixed the spraying volume at 3 mL, and the surface morphology of the composite membrane was characterized by SEM after spraying. When the concentration of the membrane-casting solution was 0.25 wt%, the surface of the composite membrane exhibited a rough texture when observed at low magnification (Fig. S1a). Zooming in further revealed that macropores were still exposed on the surface and the S2VP layer could not completely cover the PVDF substrate (Fig. S1b). When the casting solution concentration was increased to 0.5 wt% and 0.75 wt%, a complete and dense S2VP layer could be formed with no porous PVDF substrate exposed on the surface, as shown in Fig. 2 and Fig. S2. Apparently, the casting solution with a low concentration has a low viscosity and strong fluidity, when the sprayed solution reaches the surface, it may partially infiltrate into the inner pores of the PVDF substrate, leading to defective areas. As the concentration of the casting solution is increased, the enhanced viscosity limits the downward leakage of the solution, thus the intact S2VP layer can be formed. The cross-sectional SEM observation (Fig. 2c) showed the bi-layered structure with a dense S2VP layer positioned on top of the macroporous substrate. The prepared composite membrane with a size of 10 cm × 10 cm exhibited a lustrous appearance on the side coated with the S2VP layer and the opposite side remained dull (Fig. 2d and e).

Based on the macrophase separation nature, the P2VP block would form cylinders distributed in the PS matrix in the S2VP layer of the composite membrane, but the orientation of P2VP cylinders was disordered for the as-coated membrane [41,42]. Therefore, the composite membrane was exposed to a saturated chloroform vapor environment to align cylinders by annealing [43]. After getting an ordered morphology with perpendicular aligned P2VP cylinders, the membrane was executed to selective swelling to transform the cylinders into pores. After selective swelling, the membranes presented nanopores on the surface as shown in Fig. 3. For the casting solution concentration of 0.5 wt% and 0.75 wt %, the nanopores had a uniform size in a hexagonal pattern (Fig. 3a and b). However, when the concentration was increased to 1 wt%, the regularity of the pore structure was decreased, and the nanopores were no longer in a hexagonal arrangement (Fig. 3c). The cross-sectional morphology characterizations observed that the S2VP layer thicknesses of membranes prepared with S2VP concentrations of 0.5 wt% and 0.75 wt% were ~717 nm and ~1124 nm, respectively, and both of their pores were straight pores vertically through the entire layers (Figs. S3a and b). As for the solution concentration of 1 wt%, the average thickness of the S2VP layer was increased to ~2740 nm, but the cross-section exhibited a bi-continuous porous structure (Fig. S3c). The change in morphology was attributed to the excessive thickness of the S2VP layer. In the annealing process, the chloroform vapor would be difficult to uniformly penetrate in the S2VP layer to align the phase-separated structure, resulting in the inability to form vertically through pores after swelling. Under the same swelling duration of 5 h at 65 °C, the average surface pore sizes of the membranes prepared with S2VP concentrations of 0.5 wt%, 0.75 wt%, and 1 wt% were 29 nm, 31 nm, and 30 nm, respectively, implying the solution concentration, in other words, the S2VP layer thickness, has little effect on the pore size.

We noted that there were a few pores with a size much larger than the pores formed by selective swelling on the surface as circled in Figs. S4a and b. They were caused by moisture during spraying. Under a relatively high ambient humidity of 30%–50 %, the prepared membrane had much more macroporous defects on the surface (Figs. S4c and d). Controlling the humidity at 20%–30 % during spraying could inhibit the formation of macropores to a great extent, and the few ones existing almost stayed on the surface of the S2VP layer, unable to penetrate through the entire separation layer (Fig. 3e), so the separation performance of the composite membrane was unaffected.

3.2. Effects of the pore-filling agents

In addition to the membrane-casting solution concentration, the pore-filling agent should also be carefully chosen for the preparation of HOMEs. The PEG aqueous solutions with concentrations of 10 wt% and 20 wt% were first investigated. As shown in Fig. S5, the intact S2VP separation layers could be achieved, but there were only a few anomalous pores formed after selective swelling at both PEG concentrations of 10 wt% and 20 wt%, far from the hexagonally arranged pores. This result suggests the PEG solution is inappropriate to be used as the pore-filling agent. Then, we studied the effect of the PSS aqueous solution as a pore-filling agent on the membrane preparation. As shown in Fig. S6, the as-sprayed S2VP layer could cover the PVDF substrate completely without obvious defects. It was proved that the PSS pore-filling agent effectively prevented the S2VP solution from penetrating into the PVDF substrate. However, the S2VP layer failed to get an ordered homoporous structure when 10 wt% PSS aqueous solution was used, the surface of the S2VP layer had some defects of large pores, and the porosity was low (Figs. S6a and b). When the concentration of the PSS aqueous solution was increased to 20 wt%, the defects of large pores on the surface of the S2VP layer almost disappeared, and regular pores of uniform size were formed after selective swelling (Figs. S6c and d). The results indicate that the PSS solution with a low concentration is unfavorable for the preparation of HOMEs. We speculate the reason for this is the solution with a low concentration has a relatively high saturated vapor pressure of water, so the water molecules of the PSS solution filled in the substrate pores are more prone to volatilize to the S2VP layer during the spraying and annealing process, leading to the humidity defects and impacting the microphase separation morphology of S2VP. Furthermore, we examined the adhesive force between the S2VP layer and the substrate of the prepared composite membrane. Although the regular

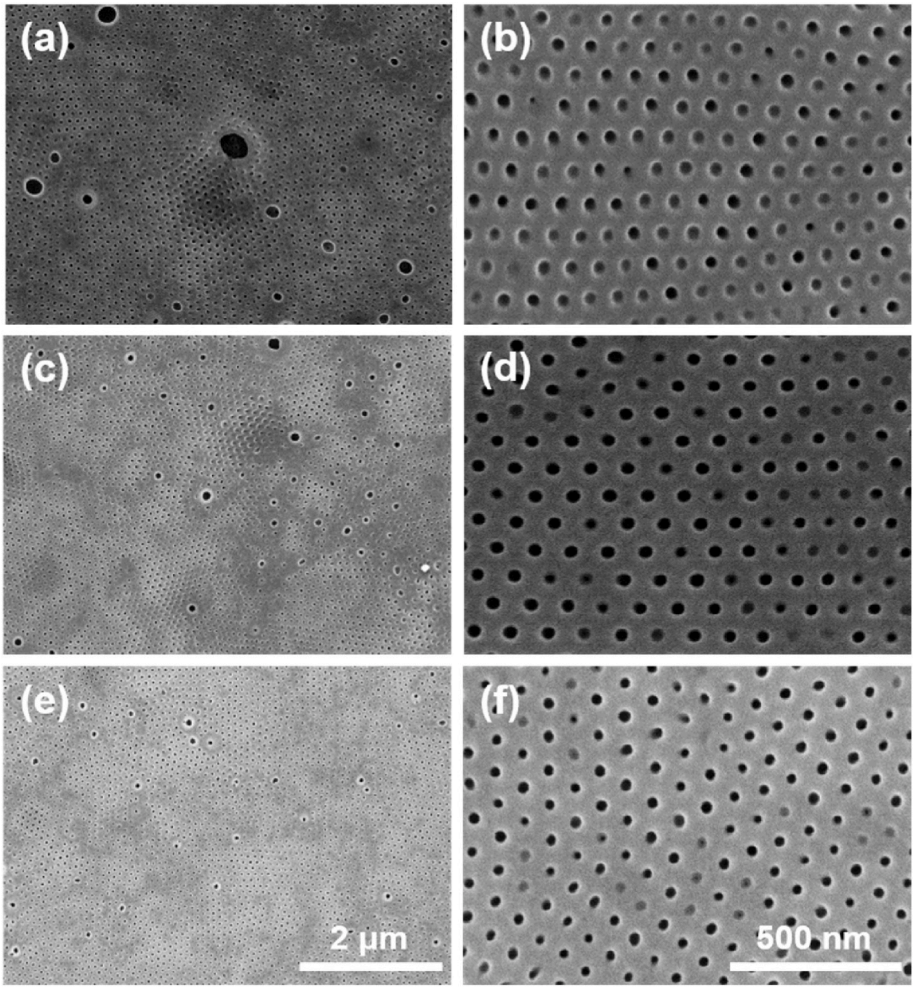

Fig. 4. Surface SEM images of membranes prepared by using the pore-filling agents of PVP aqueous solutions with different concentrations: (a, b) 5 wt%, (c, d) 10 wt %, and (e, f) 20 wt%. Images (a, c, e) and (b, d, f) have the same magnification with the scale bars corresponding to 2 μm and 500 nm provided in (e) and (f), respectively.

pores could be achieved when the PSS aqueous solution was 20 wt%, the smooth surface (Fig. S6e) of the membrane before swelling became coarse, and emerged some blisters after swelling (Fig. S6f), indicating the adhesive force between the S2VP layer and the macroporous substrate was insufficient.

In order to achieve both the homoporous structure and the robust adhesion between the S2VP layer and the substrate, the PVA and PVP aqueous solutions as the pore-filling agents were further investigated to prepare HOMEs. When a 10 wt% PVA aqueous solution was configured, we found the solution was very viscous because of the strong hydrogen bonding interactions between PVA polymer chains, resulting in poor fluidity of the solution. Using it to fill the PVDF substrate, the PVA aqueous solution was difficult to enter the PVDF substrate and fill the pores thoroughly. During the spraying process, the S2VP chloroform solution partially penetrated into the macropores of the PVDF substrate, resulting in large areas of defects (Fig. S7). When we decreased the PVA solution concentration to 5 wt%, a complete and dense S2VP layer could be obtained after spraying, and the hexagonally arranged nanopores were formed after selective swelling (Figs. 2 and 3). Moreover, there was no peeling off or blisters in the S2VP layer after the composite membrane was washed at a high temperature of 90 °C to remove the PVA pore-filling agent and swelling in 65 °C ethanol for 5 h, which indicates the S2VP layer could tightly adhere to the substrate as the 5 wt% PVA aqueous solution was used as the pore-filling agent. For the PVP aqueous solutions, HOMEs with well-defined uniform through pores could be achieved at different concentrations varying from 5 wt% to 20 wt% as shown in Fig. 4. Similar to the pore-filling agent of PSS solutions, the PVP solution with a low concentration would result in some defects of large pores on the surface of the S2VP layer. Increasing the PVP solution concentration would restrain the formation of large pores, thus the 20 wt % PVP solution produced a better homoporous structure than the 5 wt% and 10 wt% PVP solutions. Given the above, the morphology of the S2VP layer is sensitively affected by the species and the concentrations of the pore-filling agent, and 5 wt% PVA and 20 wt% PVP aqueous solutions are the preferred ones according to our experiment results.

We compared the adhesive strength of HOMEs prepared by using 5 wt% PVA and 20 wt% PVP aqueous solutions as the pore-filling agents. As shown in Fig. 5, both of the HOMEs with two kinds of pore-filling agents showed good adhesive force without obvious exfoliation or cracking on the surface after swelling. Further exposing the membranes to ultrasonic treatment, it was observed that the membrane prepared by PVP filling still did not change in appearance and no S2VP layer peeled off even after 40 min treatment, but the S2VP layer of the membrane prepared by PVA filling partly detached from the substrate after 20 min treatment (Fig. 5g) and peeled off completely after 40 min treatment (Fig. 5h). As the membrane prepared by PVA filling needed to be stirred at a high temperature of 90 °C for 3 h when removing PVA, the adhesive force between the S2VP layer and the PVDF substrate was greatly reduced. By contrast, the PVP has better water solubility and can be washed off only by stirring in pure water at room temperature.

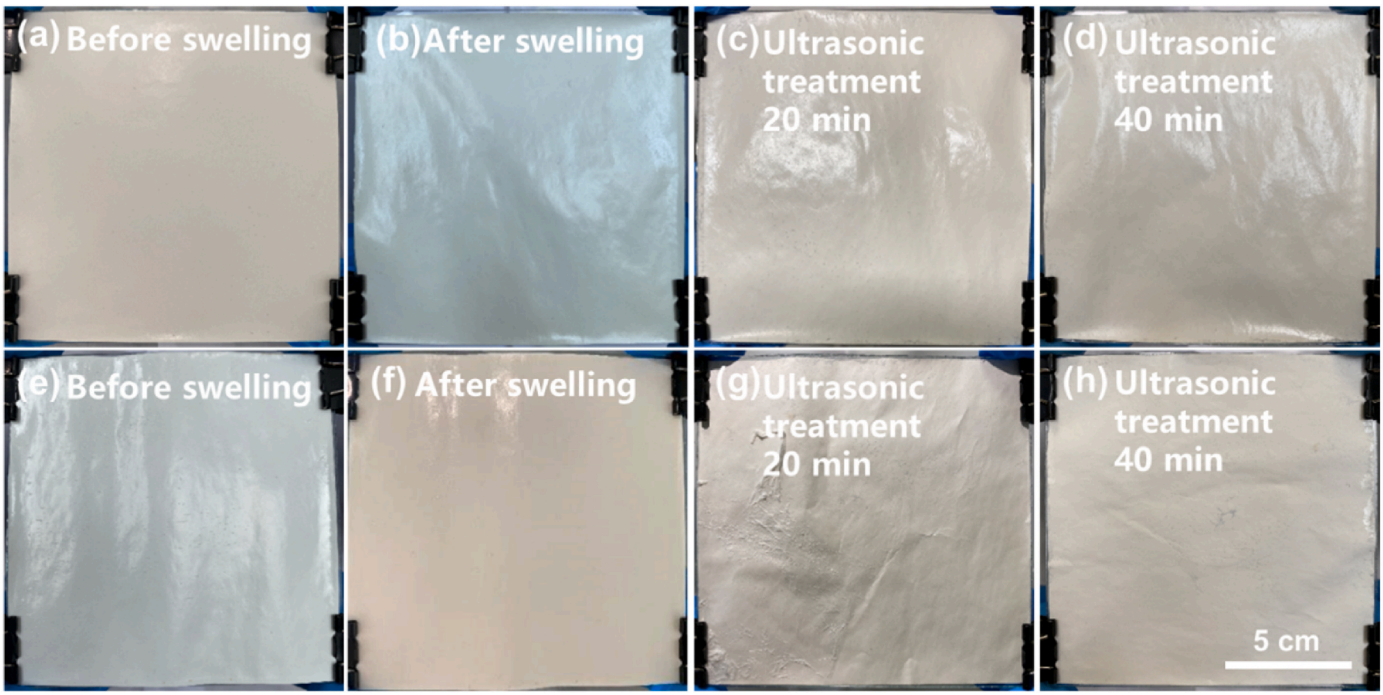

Fig. 5. Digital images of HOMEs prepared by using (a-d) the 20 wt% PVP aqueous solution and (e-h) the 5 wt% PVA aqueous solution as pore-filling agents. All images have the same magnification with a scale bar corresponding to 5 cm provided in (h).

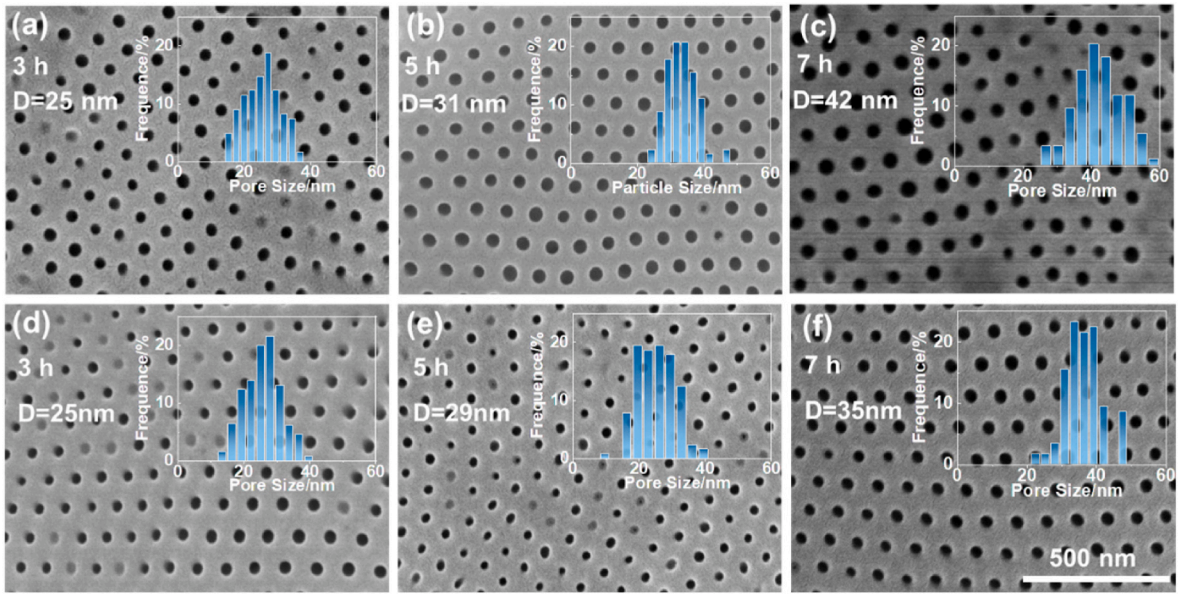

Fig. 6. Surface SEM images of composite membranes prepared by using (a-c) the 5 wt% PVA aqueous solution and (d-f) the 20 wt% PVP aqueous solution as pore-filling agents after swelling at 65 °C for different durations: (a, d) 3 h, (b, e) 5 h and (c, f) 7 h. All images have the same magnification with a scale bar corresponding to 500 nm provided in (h).

Therefore, the adhesive force of the HOME prepared by PVP filling is stronger than that of the HOME prepared by PVA filling. Also, the strong adhesion makes this HOME much more robust than that prepared via the transfer method.

3.3. Regulation of pore sizes and separation performances

The pore sizes of HOMEs could be adjusted by changing the swelling durations. The longer the swelling duration, the larger the pore size formed [44]. We investigated the pore sizes of HOMEs prepared by using 5 wt% PVA and 20 wt% PVP aqueous solutions as the pore-filling agents for different swelling durations. As shown in Fig. 6, swelling of the membranes by PVA filling for 3 h, 5 h, and 7 h resulted in pore sizes of 25 nm, 31 nm, and 42 nm, respectively, while pore sizes of the membranes by PVP filling varied from 25 nm, 29 nm–35 nm, which were smaller than the former ones although the swelling conditions were the same. This may be because the P2VP cylinders absorb ethanol and expand their volumes during swelling, and the PS phases are squeezed having to deform their matrix to form pores, however, the stronger adhesion between the S2VP layer and porous substrate for the

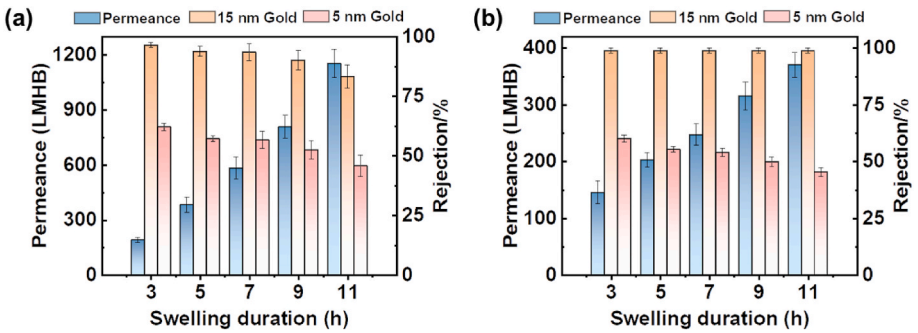

Fig. 7. The permeances and rejections to 15 nm and 5 nm gold nanoparticles across HOMEs prepared by (a) PVA filling and (b) PVP filling subjected to swelling at 60 °C for various durations. (For interpretation of the references to color in this figure legend, the reader is referred to the Web version of this article.)

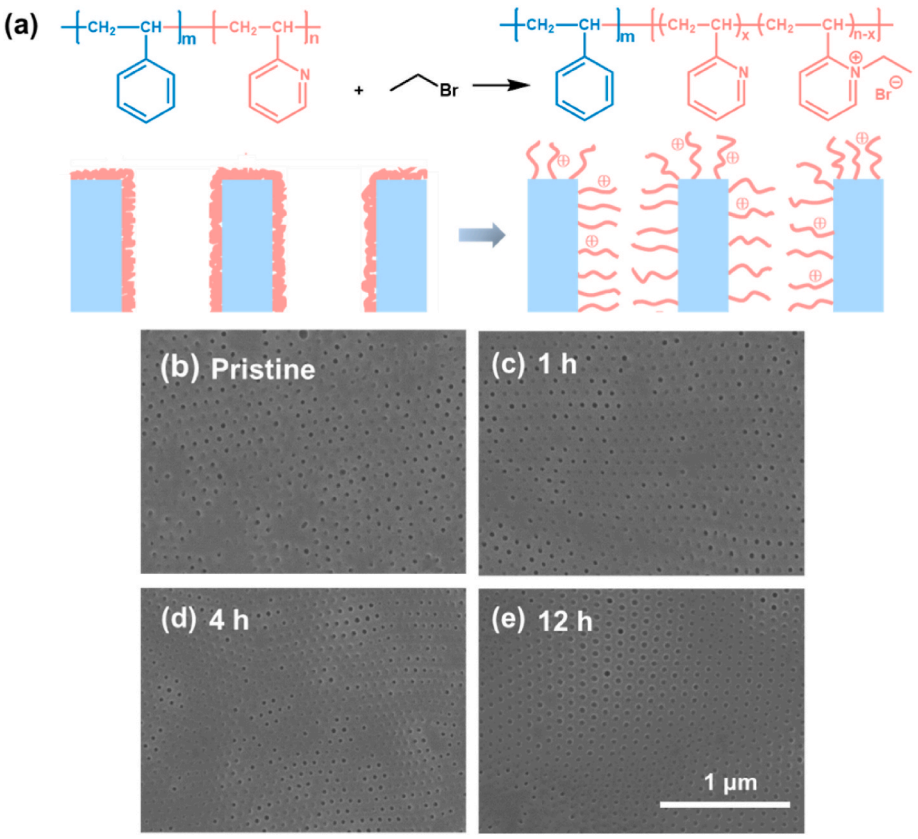

Fig. 8. (a) Schematic of the quaternization modification on HOMEs. The SEM images of the membranes (b) before and (b-e) after modification in the bromoethane-ethanol mixed solvent containing 10 % bromoethane (v/v) for different durations.

membranes by PVP filling may partially restrict the deformation of PS phases, resulting in relatively smaller pore sizes.

The pore size is closely related to the separation performance. We tested the separation performances of HOMEs prepared by PVA and PVP filling subjected to swelling for different durations. As shown in Fig. 7, with the swelling duration increased from 3, 5, 7, 9, to 11 h, the pure water permeances of HOMEs prepared by PVA filling exhibited an upward trend from 190, 382, 582, 807, to 1153 L m^{-2} h^{-1} bar^{-1} (LMHB) because of the increased pore sizes. Meanwhile, the rejections to the gold nanoparticle with a size of 15 nm were decreased from 96.1 %, 94 %, 93.6, 90.4 %, to 83.2 %, respectively, and the rejections to the 5 nm gold nanoparticle changed from 62.2 %, 56.8 %, 56.2 %, 52.3 %, to 45.8 %, respectively. Fig. S8 shows the UV–vis absorption spectrum of the 15 nm gold nanoparticle in the feed, permeation, and retentate solutions treated by the membrane subjected to 3 h swelling. The absorption peak of gold nanoparticles at 520 nm almost disappeared in the permeation solution while a significant increase in the gold concentration was noted for the retentate solution, demonstrating that the nanoparticles were effectively intercepted by the membrane based on size sieving rather than adsorption. In terms of HOMEs prepared by PVP filling, the pure water permeances were increased from 145, 202, 247, 315, to 370 LMHB as the swelling durations were prolonged from 3, 5, 7, 9 to 11 h. The rejections to 15 nm gold nanoparticles remained stable at a high level of 98.8 %, meanwhile, the rejections to 5 nm gold nanoparticles were decreased gradually from an initial value of 60 %–45.3 %. The permeances of HOMEs prepared by PVA filling were overall higher than that of HOMEs prepared by PVA filling while the rejections were lower, due to their difference in pore sizes which has been discussed above.

3.4. *Quaternization to boost performances*

Because the P2VP chains spontaneously migrate on the surface and

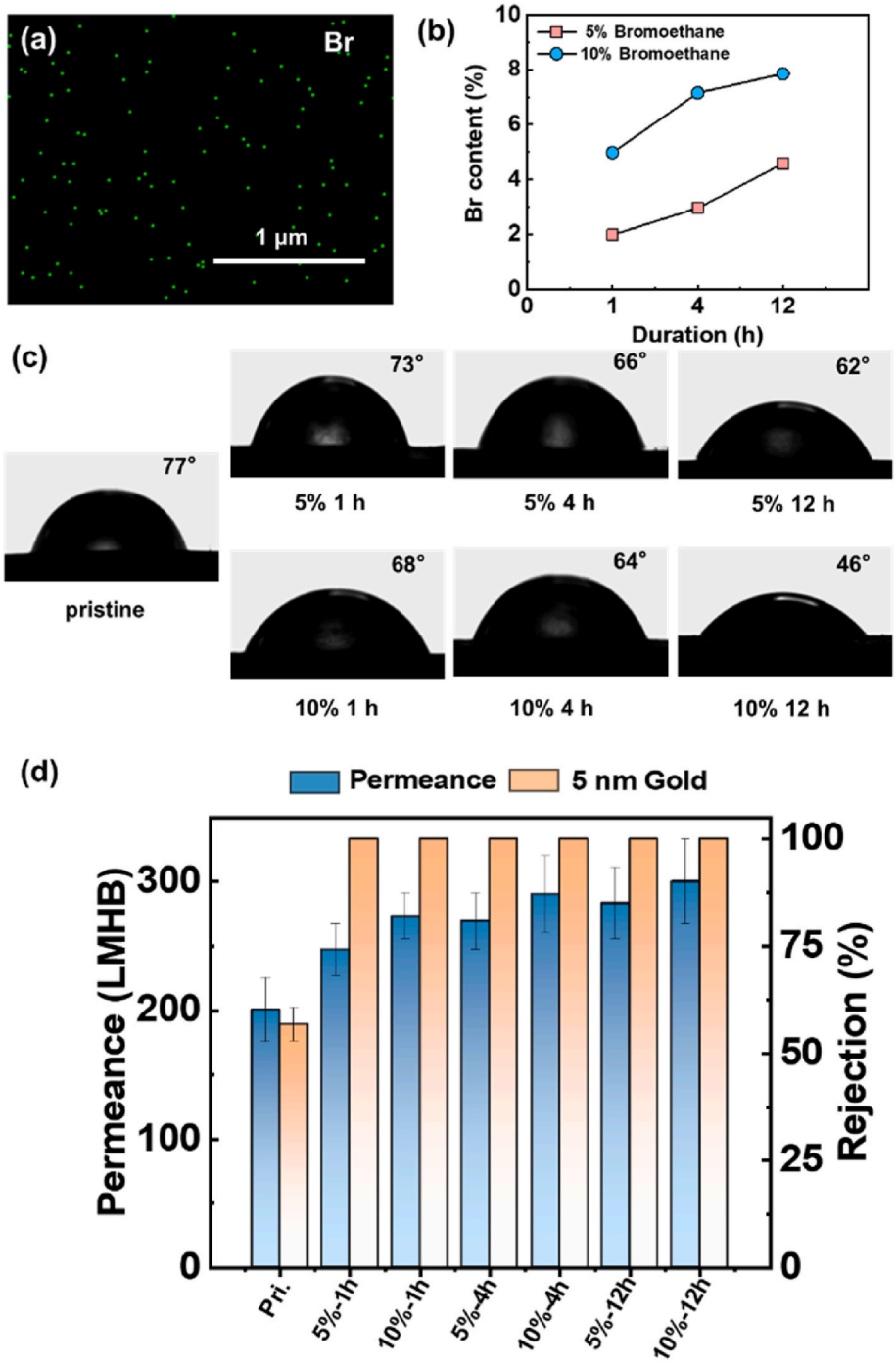

Fig. 9. (a) The surface EDX image of the HOME modified in the bromoethane-ethanol mixture containing 10 % bromoethane for 4 h. (b) The surface Br contents, (c) WCAs, and (d) separation performances of HOMEs with different modification durations in bromoethane-ethanol mixtures containing 5 % and 10 % bromoethane.

pore walls during selective swelling pore generation [45], the pyridine groups in P2VP chains provide reactive sites for further modification of the HOMEs. Therefore, we used bromoethane to react with the pyridine groups of P2VP chains to adjust the surface property and boost the separation performances of HOMEs (Fig. 8). The S2VP separation layer of the HOME before modification showed a homoporous structure (Fig. 8b). After immersing the membrane in a bromoethane-ethanol mixture containing 10 % bromoethane (v/v) for 1, 4, and 12 h, no dissolution or destruction phenomena were observed in the S2VP layer (Fig. 8c-e). The morphology was consistent with the membrane morphology before the reaction, indicating the modification of bromoethane would not change the morphology of HOMEs.

EDX was used to analyze the elementary composition on the surface of HOMEs after quaternization modification. As shown in Fig. 9a, EDX captured the distribution of bromine on the surface of the S2VP layer, thereby confirming the successful grafting of bromoethane. The grafting amounts of bromoethane were adjusted by varying the bromoethane content in the bromoethane-ethanol mixture and the modification duration. As shown in Fig. 9b, the bromine content on the S2VP layer surface was increased with longer modification durations and higher bromoethane contents. It is worth noting that bromoethane has a certain solubility to S2VP, which would cause the partial dissolution of the S2VP layer when the bromoethane content was increased to 15 %.

Since the quaternization reaction between pyridine groups and

bromoethane would change the hydrophilicity of P2VP chains of the S2VP layer, we tested the surface water contact angles (WCAs) of the membranes to observe the changes in their surface hydrophilicity before and after modification. As shown in Fig. 9c, the WCA of the original HOME was 77°, which was decreased to 73°, 66°, and 62° after modification with the bromoethane-ethanol mixed solvent containing 5 % bromoethane for 1, 4, and 12 h, respectively. As the content of bromoethane was increased to 10 %, the WCAs were reduced to 67°, 64°, and 46° after modification for 1, 4, and 12 h, respectively. The WCA test results showed that the hydrophilicity was increased with the bromoethane content and the modification duration, which could be attributed to the improved quaternization degree of P2VP chains. This finding is consistent with the experimental results obtained from EDX analysis of bromine contents.

The improved hydrophilicity of the membrane is in favor of upgrading the separation performances theoretically. Therefore, we tested the performances of the modified composite membranes, as shown in Fig. 9c. The HOME, which had a pure water permeance of 202 LMHB and a rejection to 5 nm gold nanoparticle of 55.3 % before modification, was used as the original sample. After modification with the bromoethane-ethanol mixture containing 5 % bromoethane for 1, 4, and 12 h, the permeance of the membrane was increased to 247, 269, and 283 LMHB, respectively, and the rejection to 5 nm gold nanoparticles was increased to 100 %. Increasing the bromoethane content to 10 % resulted in the increase in permeance to 273, 290, and 300 LMHB, meanwhile maintaining the rejection to 5 nm gold nanoparticles at a high rate of 100 %. The highest permeance of the modified membrane exhibited a 49 % increase compared to the original membrane. The enhanced permeance of the modified HOME is due to the improved hydrophilicity of the S2VP separation layer, and the increased rejection is attributed to the stretching of P2VP chains after the reaction between pyridine groups and bromoethane, which leads to the pore size reduction. Therefore, the modification enables the synchronous promotion of permeance and rejection for HOMEs.

4. Conclusions

In this work, we prepare HOMEs over a large area of 100 cm^2 by spray-coating S2VP onto porous substrates, followed by annealing and selective swelling processes. By precisely controlling the S2VP concentrations and ambient humidity during spray coating, thin S2VP layers without noticeable defects could be formed. Various pore-filling agents used to fill the pores of substrates are investigated, and the results indicate that the PVA aqueous solution with a concentration of 5 wt% and the PVP aqueous solution with a concentration of 20 wt% are the preferred options for producing membranes with both well-defined uniform through pores and intact composite structures. Notably, the HOMEs prepared through PVP filling exhibit robust adhesion between the S2VP layers and the porous substrates, enabling them to tolerate the ultrasonic treatment. The pore sizes as well as separation performances of HOMEs can be manipulated by adjusting the swelling durations. Profiting from the excellent structural stability as well as the P2VP chains on the surface, these membranes can be further modified using bromoethane to react with the pyridine groups of P2VP chains, resulting in the synchronous promotion of permeance and rejection. This spray-coating method exhibits significant potential for upscaling the production of HOMEs.

CRediT authorship contribution statement

Jiemei Zhou: Data curation, Investigation, Writing – original draft, Writing – review & editing. **Yifei Huang:** Data curation, Investigation. **Can Chen:** Data curation, Investigation. **Yong Wang:** Conceptualization, Funding acquisition, Supervision, Writing – review & editing.

Declaration of competing interest

The authors declare that they have no known competing financial interests or personal relationships that could have appeared to influence the work reported in this paper.

Data availability

Data will be made available on request.

Acknowledgments

Financial support from the National Natural Science Foundations of China (21825803, 21921006) is gratefully acknowledged.

Appendix A. Supplementary data

Supplementary data to this article can be found online at https://doi.org/10.1016/j.memsci.2024.122467.

References

[1] S.Y. Zhang, L. Shen, H. Deng, Q.Z. Liu, X.D. You, J.Q. Yuan, Z.Y. Jiang, S. Zhang, Ultrathin membranes for separations: a new era driven by advanced nanotechnology, Adv. Mater. 34 (2022) 2108457.
[2] S.S. Yuan, X. Li, J.Y. Zhu, G. Zhang, P. Van Puyvelde, B. Van der Bruggen, Covalent organic frameworks for membrane separation, Chem. Soc. Rev. 48 (2019) 2665–2681.
[3] A. Lee, J.W. Elam, S.B. Darling, Membrane materials for water purification: design, development, and application, Envion. Sci.: Water Res. Technol. 2 (2016) 17–42.
[4] R.Z. Waldman, F. Gao, W.A. Phillip, S.B. Darling, Maximizing selectivity: an analysis of isoporous membranes, J. Membr. Sci. 633 (2021) 119389.
[5] Z. Shu, H.Z. Li, Y. Shi, D.Y. Zuo, Z. Yi, C.J. Gao, Dual sugar and temperature responsive isoporous membranes for protein sieving with improved separation coefficient and decreased denaturation, J. Membr. Sci. 672 (2023) 121450.
[6] Y. Wang, Nondestructive creation of ordered nanopores by selective swelling of block copolymers: toward homoporous membranes, Acc. Chem. Res. 49 (2016) 1401–1408.
[7] J.M. Zhou, Y. Wang, Selective swelling of block copolymers: an upscalable greener process to ultrafiltration membranes? Macromolecules 53 (2020) 5–17.
[8] E.A. Jackson, M.A. Hillmyer, Nanoporous membranes derived from block copolymers: from drug delivery to water filtration, ACS Nano 4 (2010) 3548–3553.
[9] A. Saxena, B.P. Tripathi, M. Kumar, V.K. Shahi, Membrane-based techniques for the separation and purification of proteins: an overview, Adv. Colloid Interface Sci. 145 (2009) 1–22.
[10] P. Kosiol, M.T. Muller, B. Schneider, B. Hansmann, V. Thom, M. Ulbricht, Determination of pore size gradients of virus filtration membranes using gold nanoparticles and their relation to fouling with protein containing feed streams, J. Membr. Sci. 548 (2018) 598–608.
[11] A. Sabirova, F. Pisig, N. Rayapuram, H. Hirt, S.P. Nunes, Nanofabrication of isoporous membranes for cell fractionation, Sci. Rep. 10 (2020) 6138.
[12] D.A. Olson, L. Chen, M.A. Hillmyer, Templating nanoporous polymers with ordered block copolymers, Chem. Mater. 20 (2008) 869–890.
[13] V. Abetz, Isoporous block copolymer membranes, Macromol. Rapid Commun. 36 (2015) 10–22.
[14] S.P. Nunes, Block copolymer membranes for aqueous solution applications, Macromolecules 49 (2016) 2905–2916.
[15] Y.D. Luo, D. Montarnal, S. Kim, W.C. Shi, K.P. Barteau, C.W. Pester, P.D. Hustad, M.D. Christianson, G.H. Fredrickson, E.J. Kramer, C.J. Hawker, Poly (dimethylsiloxane-*b*-methyl methacrylate): a promising candidate for sub-10 nm patterning, Macromolecules 48 (2015) 3422–3430.
[16] S.S. Xiong, D.X. Li, S.M. Hur, G.S.W. Craig, C.G. Arges, X.P. Qu, P.F. Nealey, The solvent distribution effect on the self-assembly of symmetric triblock copolymers during solvent vapor annealing, Macromolecules 51 (2018) 7145–7151.
[17] D. Borah, R. Senthamaraikannan, S. Rasappa, B. Kosmala, J.D. Holmes, M. A. Morris, Swift nanopattern formation of PS-*b*-PMMA and PS-*b*-PDMS block copolymer films using a microwave assisted technique, ACS Nano 7 (2013) 6583–6596.
[18] K.W. Tan, B. Jung, J.G. Werner, E.R. Rhoades, M.O. Thompson, U. Wiesner, Transient laser heating induced hierarchical porous structures from block copolymer-directed self-assembly, Science 349 (2015) 54–58.
[19] I. Gunkel, Directing block copolymer self-assembly on patterned substrates, Small 14 (2018) e1802872.
[20] Y. Mai, A. Eisenberg, Self-assembly of block copolymers, Chem. Soc. Rev. 41 (2012) 5969–5985.
[21] J. Diaz, M. Pinna, C. Breen, A. Zvelindovsky, I. Pagonabarraga, Block copolymer nanocomposites under confinement: effect on frustrated phases, Macromolecules 56 (2023) 5010–5021.

[22] N. Hampu, J.R. Werber, W.Y. Chan, E.C. Feinberg, M.A. Hillmyer, Next-generation ultrafiltration membranes enabled by block polymers, ACS Nano 14 (2020) 16446–16471.
[23] R. Milani, N. Houbenov, F. Fernandez-Palacio, G. Cavallo, A. Luzio, J. Haataja, G. Giancane, M. Saccone, A. Priimagi, P. Metrangolo, O. Ikkala, Hierarchical self-assembly of halogenbonded block copolymer complexes into upright cylindrical domains, Chem 2 (2017) 417–426.
[24] A. Sarkar, M. Stefik, Robust porous polymers enabled by a fast trifluoroacetic acid etch with improved selectivity for polylactide, Mater. Chem. Front. 1 (2017) 1526–1533.
[25] A. Bertrand, M.A. Hillmyer, Nanoporous poly(lactide) by olefin metathesis degradation, J. Am. Chem. Soc. 135 (2013) 10918–10921.
[26] A. Vora, B. Zhao, D. To, J.Y. Cheng, A. Nelson, Blends of PS-PMMA diblock copolymers with a directionally hydrogen bonding polymer additive, Macromolecules 43 (2010) 1199–1202.
[27] K.L. Sedransk, A.C. Fisher, G.D. Moggridge, Development of porous thin film polymers using metathetic etching on block copolymers, Mater. Lett. 145 (2015) 299–303.
[28] C. Zhou, T. Segal-Peretz, M.E. Oruc, H.S. Suh, G.P. Wu, P.F. Nealey, Fabrication of nanoporous alumina ultrafiltration membrane with tunable pore size using block copolymer templates, Adv. Funct. Mater. 27 (2017) 1701756.
[29] E. Cara, I. Murataj, G. Milano, N. De Leo, L. Boarino, F. Ferrarese Lupi, Recent advances in sequential infiltration synthesis (SIS) of block copolymers (BCPs), Nanomaterials 11 (2021) 994.
[30] X.B. Yang, A.B.F. Martinson, J.W. Elam, L. Shao, S.B. Darling, Water treatment based on atomically engineered materials: atomic layer deposition and beyond, Matter 4 (2021) 3515–3548.
[31] Y. Wang, F.B. Li, Pore-making strategy: confined swelling induced pore generation in block copolymer materials, Adv. Mater. 23 (2011) 2134–2148.
[32] S.T. Qiu, Z. Li, X.Y. Ye, X. Ying, J.M. Zhou, Y. Wang, Selective swelling of polystyrene (PS)/poly(dimethylsiloxane) (PDMS) block copolymers in alkanes, Macromolecules 56 (2023) 215–225.
[33] Y.J. Wang, C.X. Zhang, J.M. Zhou, Y. Wang*, Room-temperature swelling of block copolymers for nanoporous membranes with well-defined porosities, J. Membr. Sci. 608 (2020) 118186.
[34] L.M. Guo, Z.G. Wang, Y. Wang, Perpendicular alignment and selective swelling-induced generation of homopores of polystyrene-b-poly(2-vinylpyridine)-b-poly (ethylene oxide) triblock terpolymer, Macromolecules 51 (2018) 6248–6256.
[35] R. John, K. Pal, J.S. Jayan, S. Appukuttan, K. Joseph, New emerging review on advances in block copolymer based water purification membranes, J. Mol. Struct. 1231 (2021) 129926.
[36] C. Zhou, T. Segal-Peretz, M.E. Oruc, H.S. Suh, G.P. Wu, P.F. Nealey, Fabrication of nanoporous alumina ultrafiltration membrane with tunable pore size using block copolymer templates, Adv. Funct. Mater. 27 (2017) 1701756.
[37] J.W. Lee, J.H. Kim, D.J. An, J.K. Lee, N. Kim, S.H. Kim, Mesoporous composite membrane based on block copolymer self-assembly, Macromol. Res. 27 (2019) 974–981.
[38] E.J. Vriezekolk, T. Kudernac, W.M. de Vos, K. Nijmeijer, Composite ultrafiltration membranes with tunable properties based on a self-assembling block copolymer/homopolymer system, J. Polym. Sci., Part B: Polym. Phys. 53 (2015) 1546–1558.
[39] Z. Zhang, C. Chen, S.S. Zhang, X.Y. Ye, J.M. Zhou, Y. Wang, Large-area homoporous membranes (HOMEs) enabled by multiple annealing, J. Membr. Sci. 662 (2022) 121021.
[40] X.S. Shi, Z.G. Wang, Y. Wang, Highly permeable nanoporous block copolymer membranes by machinecasting on nonwoven supports: an upscalable route, J. Membr. Sci. 533 (2017) 201–209.
[41] W.A. Phillip, M.A. Hillmyer, E.L. Cussler, Cylinder orientation mechanism in block copolymer thin films upon solvent evaporation, Macromolecules 43 (2010) 7763–7770.
[42] K.A. Cavicchi, T.P. Russell, Solvent annealed thin films of asymmetric polyisoprene-polylactide diblock copolymers, Macromolecules 40 (2007) 1181–1186.
[43] S.H. Kim, M.J. Misner, T. Xu, M. Kimura, T.P. Russell, Highly oriented and ordered arrays from block copolymers via solvent evaporation, Adv. Mater. 16 (2004) 226–231.
[44] M.J. Wei, W. Sun, X.S. Shi, Z.G. Wang, Y. Wang, Homoporous membranes with tailored pores by soaking block copolymer/homopolymer blends in selective solvents: dissolution versus swelling, Macromolecules 49 (2016) 215–223.
[45] Z.G. Wang, X.P. Yao, Y. Wang, Swelling-induced mesoporous block copolymer membranes with intrinsically active surfaces for size-selective separation, J. Mater. Chem. 22 (2012) 20542–20548.